

Detection of Large Scale Structure in a $B < 17^m$ Galaxy Redshift Survey.

A. Ratcliffe*, T. Shanks*, A. Broadbent*, Q.A. Parker†,

F.G. Watson†, A.P. Oates‡, R. Fong* & C.A. Collins§

**Physics Dept., Univ. of Durham, South Road, Durham, DH1 3LE, U.K.*

†Anglo-Australian Observatory, Coonabarabran, NSW 2357, Australia.

‡Royal Greenwich Observatory, Madingley Road, Cambridge, CB3 0HA, U.K.

§Astrophysics Group, Liverpool-John-Moores Univ., Liverpool, L3 3AF, U.K.

We report on results from the Durham/UKST Galaxy Redshift Survey where we have found large scale “cellular” features in the galaxy distribution. These have spatial 2-point correlation function power significantly in excess of the predictions of the standard cold dark matter cosmological model¹, supporting the previous observational results from the APM survey^{2,3}. At smaller scales, the 1-D pairwise galaxy velocity dispersion is measured to be 387_{-62}^{+96} kms⁻¹ which is also inconsistent with the prediction of the standard cold dark matter model¹. Finally, the survey has produced the most significant detection yet of large scale redshift space distortions due to dynamical infall of galaxies⁴. An estimate of $\Omega^{0.6}/b = 0.55 \pm 0.12$ is obtained which is consistent either with a low density Universe or a critical density Universe where galaxies are biased tracers of the mass.

The principal aims of the Durham/UKST Galaxy Redshift Survey are to investigate

the structure and dynamics of the Universe on scales $1\text{--}100h^{-1}\text{Mpc}$ (where h is Hubble’s constant in units of $100\text{ kms}^{-1}\text{ Mpc}^{-1}$). The survey was constructed by measuring the redshifts for 1 in 3 of the galaxies from the Edinburgh/Durham Southern Galaxy Catalogue⁵ (EDSGC) to $b_J \simeq 17^m$. The resulting survey contains ~ 2500 redshifts, covers a $\sim 20^\circ \times 75^\circ$ contiguous area of the sky at the South Galactic Pole and probes to a depth of $> 300h^{-1}\text{Mpc}$ with a median depth of $\sim 150h^{-1}\text{Mpc}$. The total volume of space surveyed is $\sim 4 \times 10^6 h^{-3}\text{Mpc}^3$, approximately six times that of the updated Southern Sky Redshift Survey⁶, due to our $\sim 2.5^m$ fainter limit.

Figure 1 shows the distribution of the galaxies in right ascension and velocity for each of four, 5° , declination slices. The survey gives the striking impression that the galaxy distribution is “cellular” or “bubble-like” on $50\text{--}100h^{-1}\text{Mpc}$ scales. The most noticeable structure is the low density region lying between 0 and $90h^{-1}\text{Mpc}$ surrounded by long “walls” of galaxies. This structure is present in the slices at -30° , -35° and -40° and was referred to as the Sculptor Void in earlier, shallower surveys^{7,8}. In the most northerly slice at -25° there is evidence that we are seeing the top of this structure and that it is indeed a “cell”. Figure 2 shows the histogram of galaxy number with distance which has several large peaks, also indicating the presence of large scale structure. However, it should be noted that at least one of these peaks (eg. at $\sim 90h^{-1}\text{Mpc}$) does not follow the $128h^{-1}\text{Mpc}$ periodic pattern previously claimed⁹ along the North–South Galactic Pole axis which intersects our survey at $\sim 0^h54^m$, -27.5° , crossing the nearer and further Sculptor superclusters. Figure 1 clearly reveals a galaxy distribution that is more complex than any simple periodic pattern.

To test the significance of these large scale features, we have made a statistical investi-

gation of the galaxy distribution in the Durham/UKST survey by calculating the redshift space 2-point correlation function¹⁰, $\xi(s)$. This is a measure of the excess probability of finding two galaxies in given volume elements at separations s over what is expected for a homogeneous galaxy distribution. In figure 3a we compare the Durham/UKST $\xi(s)$ with that from other optical redshift surveys^{3,11,12}. On small scales ($< 10h^{-1}\text{Mpc}$) we see that there is good agreement between all the surveys. On large scales ($> 10h^{-1}\text{Mpc}$) we see that our new estimate is consistent with the detection of large scale power from the APM-Stromlo survey but less consistent with the previous Durham surveys. This inconsistency is thought to be partly statistical and partly due to the previous use of a simple unweighted estimator which, although having minimum errors, was systematically biased against the detection of large scale power (Ratcliffe *et al.*, in preparation). Our new estimate is also consistent with that found from the QDOT infrared redshift survey¹³. Figure 3b shows the Durham/UKST $\xi(s)$ with the results from mock catalogues drawn from two sets of cold dark matter¹ (CDM) N-body simulations^{14,15,16}; standard CDM with $\Omega h = 0.5$, $b = 1.6$ (SCDM) and CDM with $\Omega h = 0.2$, $b = 1$ and a cosmological constant ($\Lambda \neq 0$) to ensure a spatially flat cosmology (LCDM), where Ω is the mean mass density of the Universe and b is the linear bias parameter relating the galaxy and underlying matter distributions, $(\Delta\rho/\rho)_g = b(\Delta\rho/\rho)_m$. The mock catalogues were constructed with the same angular and radial selection functions as the Durham/UKST survey. On small scales ($< 10h^{-1}\text{Mpc}$) both CDM models agree well with the data. On large scales ($> 10h^{-1}\text{Mpc}$) SCDM shows no significant large scale power whereas LCDM shows significant power out to $\sim 30h^{-1}\text{Mpc}$. The data therefore shows significant excess power at $\sim 15\text{-}30h^{-1}\text{Mpc}$ over SCDM ($> 3\sigma$). LCDM is more consistent with the data at these scales, although even this model produces

too little power at the 2σ level. This rejection of SCDM in our new survey is consistent with the findings from the APM correlation functions^{2,3}.

Inferring galaxy distances from redshifts results in the distortion of the clustering pattern because of the non-Hubble component of galaxy velocities. This anisotropy along the line of sight can be used to estimate some important cosmological parameters describing the dynamics of the Universe^{4,10}. Figure 4a shows a contour plot of the 2-point correlation function, $\xi_v(\sigma, \pi)$, where σ and π are the perpendicular and parallel separations to the line of sight, respectively. On small, non-linear scales the contours are elongated parallel to the line of sight caused by the rms virial velocities of galaxies. Using standard techniques¹⁰ to model this smearing of ξ by the peculiar velocities, we find $\langle v^2 \rangle^{\frac{1}{2}} = 387_{-62}^{+96}$ kms⁻¹ at perpendicular separations $\sigma < 2h^{-1}$ Mpc. Assuming that simple biasing models apply¹⁷, this is inconsistent with the SCDM prediction¹ of ~ 1000 kms⁻¹ but nearer the LCDM prediction¹ of ~ 600 kms⁻¹. On large, linear scales the contours are compressed parallel to the line of sight caused by the infall of galaxies into overdense regions. We use two independent methods to estimate $\Omega^{0.6}/b$ as shown in figure 4b. Firstly, using the spherical harmonic moments¹⁸ ($\tilde{\xi}$) of $\xi_v(\sigma, \pi)$ to measure the shape of the contours of constant ξ , we find $\Omega^{0.6}/b = 0.55 \pm 0.12$ in the region $9-23h^{-1}$ Mpc. Secondly, using the enhancement in redshift space⁴ of the volume integral of ξ (J_3) over the real space one, we find $\Omega^{0.6}/b = 0.48 \pm 0.18$, quoting the result at $10h^{-1}$ Mpc, which is representative. Our measured values of $\Omega^{0.6}/b$ can be compared with other optical values of $\Omega^{0.6}/b$ estimated from redshift space distortions, namely 0.48 ± 0.12 (Loveday *et al.*, manuscript submitted), 0.77 ± 0.16 ¹⁹ and 0.5 ± 0.25 ²⁰. All of these values agree within 2σ of our results. Thus taking two fiducial values for b , $b = 1$ implies $\Omega = 0.37 \pm 0.15$ and $b = 2$ implies $\Omega = 1.17 \pm 0.31$. This result

tends to argue against an unbiased critical density, $\Omega = 1$, Universe, but favours a biased, $\Omega = 1$, Universe or an unbiased, low Ω , Universe.

Thus our $\Omega^{0.6}/b$ result agrees with the SCDM and LCDM models but, since they both predict $\Omega^{0.6}/b \sim 0.4-0.6$, we cannot discriminate between them. However, we have shown that SCDM underpredicts our 2-point correlation function results at large scales and overpredicts the 1-D pairwise velocity dispersion at small scales. Therefore, overall, our results argue for a model with a density perturbation spectrum more skewed towards large scales, such as LCDM.

Acknowledgements.

We are grateful to the staff at the UKST and AAO for their assistance in the gathering of the observations. S.M. Cole, C.M. Baugh and V.R. Eke are thanked for useful discussions and supplying the CDM simulations. PPARC are thanked for allocating the observing time via PATT and for the use of the STARLINK computer facilities.

References

¹ Davis, M., Efstathiou, G., Frenk, C.S. & White, S.D.M. *Astrophys. J.* **292**, 371–394 (1985).

² Maddox, S.J., Efstathiou, G., Sutherland, W.J. & Loveday, J. *Mon. Not. R. astr. Soc.* **242**, 43p–47p (1990).

³ Loveday, J., Efstathiou, G., Peterson, B.A. & Maddox, S.J. *Astrophys. J. Lett.* **400**, L43–L46 (1992).

⁴ Kaiser, N. *Mon. Not. R. astr. Soc.* **227**, 1–21 (1987).

⁵ Collins, C.A., Heydon-Dumbleton, N.H., & MacGillivray, H.T. *Mon. Not. R. astr. Soc.* **236**, 7p–12p (1988).

⁶ Marzke, R.O., Geller, M.J., da Costa, L.N. & Huchra, J.P. *Astron. J.* **110**, 477–501 (1995).

⁷ da Costa, L.N., Pellegrini, P.S., Davis, M., Meiksin, A., Sargent, W.L. & Tonry, J.L. *Astrophys. J. Suppl. Ser.* **75**, 935–964 (1991).

⁸ Fairall, A.P. & Jones, A. *Publ. Dept. Astr. Cape Town* **10** (1988).

⁹ Broadhurst, T.J., Ellis, R.S., Koo, D.C. & Szalay, A.S. *Nature* **343**, 726–728 (1990).

¹⁰ Peebles, P.J.E. *‘The Large-Scale Structure of the Universe’*, Princeton University Press, Princeton, US (1980).

¹¹ Shanks, T., Bean, A.J., Efstathiou, G., Ellis, R.S., Fong, R., & Peterson, B.A. *Astrophys. J.* **274**, 529–533 (1983).

- ¹² Shanks, T., Hale-Sutton, D., Fong, R. & Metcalfe, N. *Mon. Not. R. astr. Soc.* **237**, 589–610 (1989).
- ¹³ Saunders, W., Frenk, C.S., Rowan-Robinson, M., Efstathiou, G., Lawrence, A., Kaiser, N., Ellis, R.S., Crawford, J., Xia, X.-Y. & Parry, I. *Nature* **349**, 32–38 (1991).
- ¹⁴ Efstathiou, G., Davis, M., Frenk, C.F. & White, S.D.M. *Astrophys. J. Suppl. Ser.* **57**, 241–260 (1985).
- ¹⁵ Couchman, H.M.P. *Astrophys. J. Lett.* **368**, L23–L26 (1991).
- ¹⁶ Gaztañaga & Baugh, C.M. *Mon. Not. R. astr. Soc.* **273**, 1p–6p (1995).
- ¹⁷ Bardeen, J.M., Bond, J.R., Kaiser, N. & Szalay, A.S. *Astrophys. J.* **304**, 15–61 (1986).
- ¹⁸ Hamilton, A.J.S. *Astrophys. J. Lett.* **385**, L5–L8 (1992).
- ¹⁹ Peacock, J.P. & Dodds, S.J. *Mon. Not. R. astr. Soc.* **267**, 1020–1034 (1994).
- ²⁰ Lin, H. *Ph.D. Thesis*, University of Harvard (1995).

²¹ Parker, Q.A. & Watson, F.G. in ‘*Wide Field Spectroscopy and the Distant Universe*’, 35th Hermonceux Conference, Cambridge, UK, (eds. Maddox, S.J. & Aragón-Salamanca, A.), World Scientific Publishing, 33–39 (1995).

²² Peterson, B.A., Ellis, R.S., Efstathiou, G.P., Shanks, T., Bean, A.J., Fong, R., & Zen-Long, Z. *Mon. Not. R. astr. Soc.* **221**, 233–255 (1986).

²³ Metcalfe, N., Fong, R., Shanks, T. & Kilkenny, D. *Mon. Not. R. astr. Soc.* **236**, 207–234 (1989).

²⁴ Hamilton, A.J.S. *Astrophys. J.* **417**, 19–35 (1993).

²⁵ Efstathiou, G. in ‘*Comets to Cosmology*’, 3rd IRAS Conference, London, UK, (ed. Lawrence, A.), Springer-Verlag, 312–319 (1988).

²⁶ Saunders, W., Rowan-Robinson, M. & Lawrence, A. *Mon. Not. R. astr. Soc.* **258**, 134–146 (1992).

Figure 1.

Redshift cone-plots of the galaxy distribution in the four contiguous 5° declination strips from the Durham/UKST redshift survey, (a), (b), (c) and (d), respectively. Large “cellular” structures in the galaxy distribution on scales of $50\text{-}100h^{-1}\text{Mpc}$ are clearly seen. The redshifts of these galaxies were obtained over the three year period 1991-1994 using the 1.2m UK Schmidt Telescope at Siding Spring, Australia, in conjunction with the fibre-coupled spectroscopy system FLAIR²¹. The completeness is $> 75\%$ to the nominal magnitude limit of $b_J = 17.0^m$. Our magnitude limit varies slightly ($0.1^m\text{-}0.2^m$) from field to field but this is exactly taken into account in all our statistical analysis. A comparison of 150 galaxies with published velocities^{7,8,22,23} indicates that our measurements have a negligible offset and are accurate to $\pm 150 \text{ kms}^{-1}$ (Ratcliffe *et al.* , in preparation).

Figure 2.

The histogram of galaxy number with distance, $n(r)$, in the Durham/UKST survey. The dashed curve shows how a random and homogeneous distribution would appear given our angular/radial selection functions, sampling rate and galaxy luminosity function from the Durham/UKST survey (Ratcliffe *et al.* , in preparation). The arrows indicate where the $128h^{-1}\text{Mpc}$ “spikes” in the galaxy distribution⁹ should appear in this region of the sky. In this larger angle survey the galaxy distribution clearly appears more complex than any simple periodic pattern. There are two strong peaks at ~ 90 and $\sim 170h^{-1}\text{Mpc}$ signifying “walls” in the galaxy distribution. There is possible evidence for a third such feature at $\sim 270h^{-1}\text{Mpc}$.

Figure 3.

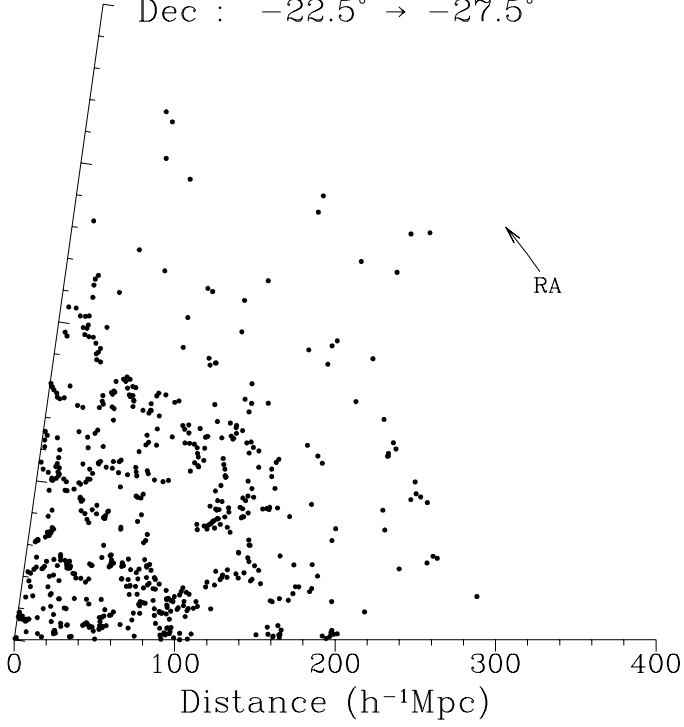
In (a) we compare the Durham/UKST 2-point correlation function, $\xi(s)$, with that from other optical redshift surveys^{3,11,12}. $\xi(s)$, was calculated using the weighted estimator^{24,25} which gave no systematic offset and the minimum variance in the CDM mock catalogues. On this plot the error bars for the Durham/UKST survey were calculated using the 1σ variance from the LCDM mock catalogues. In (b) we compare with a SCDM model and a LCDM model. The shaded areas are the 1σ confidence regions on an individual mock catalogue for the above two models of CDM using the aforementioned optimal estimator and weighting combination so that a direct comparison between the data and models can be made. We have also estimated the integral constraint to see if it would cause any systematic offset in $\xi(s)$ on large scales and find this to be a negligible effect.

Figure 4.

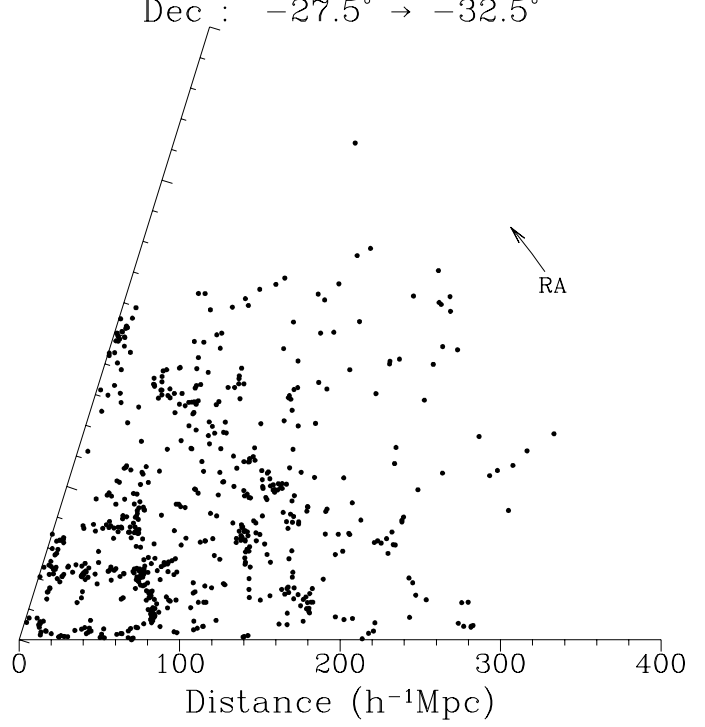
In (a) we show the contours of constant 2-point correlation function where the effects of small and large scale redshift space distortions are clearly seen. Solid lines denote $\xi > 1$ with $\Delta\xi = 1$, short dashed lines denote $0 < \xi < 1$ with $\Delta\xi = 0.1$ and long dashed lines denote $\xi < 0$ with $\Delta\xi = 0.1$. For reference, the lines with $\xi = 1$ and $\xi = 0$ are in thick bold and the regularly spaced thin bold lines show an isotropic correlation function for comparison. A representative error bar is also plotted. In this plot $\xi_v(\sigma, \pi)$ was calculated using a single pair weighting of galaxies¹⁰ because this weighting produced less noise in $\xi_v(\sigma, \pi)$. Our consistent use of this different weighting scheme has no effect on the either method of estimating $\Omega^{0.6}/b$ (Ratcliffe, *et al.* in preparation). In (b) we show our estimated values of $\Omega^{0.6}/b$ for two methods^{18,4} as a function of separation r . The solid line shows

the maximum likelihood fit for $\Omega^{0.6}/b$ to the first method of estimation ($\tilde{\xi}$) in the region $9-23h^{-1}\text{Mpc}$ and the dashed lines denote the 1σ confidence intervals of this fit. The error bars on these independent points come from the LCDM mock catalogues. The error bar of the estimated point at $\sim 10h^{-1}\text{Mpc}$ from the second method (J_3) is representative of the errors from this method and was calculated from the variance between the 4 quadrants of the survey. Only one error bar is shown because of the non-independence of the points in this method. Both of these sets of error bars include the contribution from cosmic variance. We have estimated ξ in real space using two methods involving the inversion of the projected correlation function²⁶ (Ratcliffe *et al.* , in preparation) and find consistent results.

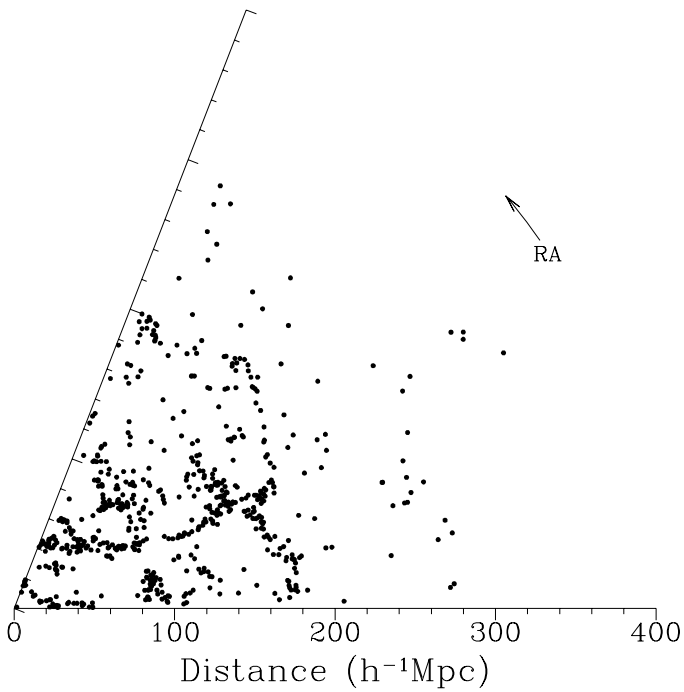
RA : $21^{\text{h}}27^{\text{m}}00^{\text{s}} \rightarrow 03^{\text{h}}29^{\text{m}}00^{\text{s}}$
Dec : $-22.5^{\circ} \rightarrow -27.5^{\circ}$



RA : $21^{\text{h}}39^{\text{m}}30^{\text{s}} \rightarrow 03^{\text{h}}15^{\text{m}}30^{\text{s}}$
Dec : $-27.5^{\circ} \rightarrow -32.5^{\circ}$



RA : $21^{\text{h}}48^{\text{m}}00^{\text{s}} \rightarrow 03^{\text{h}}24^{\text{m}}00^{\text{s}}$
Dec : $-32.5^{\circ} \rightarrow -37.5^{\circ}$



RA : $21^{\text{h}}53^{\text{m}}00^{\text{s}} \rightarrow 03^{\text{h}}41^{\text{m}}00^{\text{s}}$
Dec : $-37.5^{\circ} \rightarrow -42.5^{\circ}$

